

Electronic Supplementary Information for Thermochromic Discotic 6-Oxoverdazyls

Aleksandra Jankowiak,^a Damian Pociecha,^b Hirosato Monobe,^c Jacek Szczytko,^d and
Piotr Kaszyński*^{a,e}

^a *Organic Materials Research Group*, Department of Chemistry, Vanderbilt University,
Nashville, TN 37235, USA

^b Department of Chemistry, University of Warsaw, Żwirki i Wigury 101, 02-089
Warsaw, Poland

^c *Research Institute for Ubiquitous Energy Devices*, National Institute of Advanced
Industrial Science and Technology, AIST Kansai Centre, Ikeda, Osaka 563-8577, Japan

^d *Institute of Experimental Physics*, Faculty of Physics, University of Warsaw, Hoża 69,
00-681 Warsaw, Poland

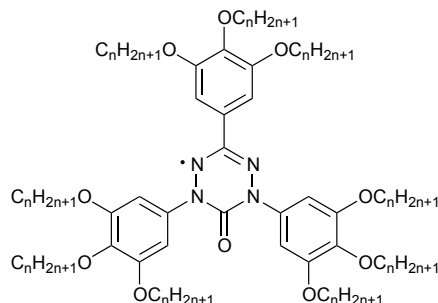
^e Faculty of Chemistry, University of Łódź, Tamka 12, 91403 Łódź, Poland

Table of Content:

1. Synthetic detailsS2
2. Thermal analysisS6
3. Optical texturesS7
4. Electronic absorption spectraS7
5. Powder XRD measurementsS8
6. Photoconductivity measurements and dataS10
7. Magnetization measurementsS12
8. ElectrochemistryS14
9. Molecular modeling and computational detailsS14
10. Disproportionation energyS15
11. Partial data for TD-DFT calculation (B3LYP/6-31G(d,p)) for 1b[1]S16
12. Archive data for B3LYP/6-31G(d,p) optimizations of 1b[1]S19
13. ReferencesS20

1. Synthetic Details

Reagents and solvents were obtained commercially. Reactions were carried out under Ar, and subsequent manipulations were conducted in air. ^1H NMR spectra were obtained at 400 MHz (^1H) in CDCl_3 and referenced to the solvent unless stated otherwise.

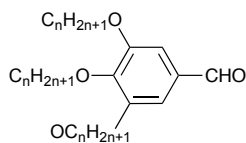


6-Oxoverdazyls 1[n]. General procedure. Method A. A mixture of crude tetrazane **6b[n]** (0.1 mmol), anhydrous Na_2CO_3 (127 mg, 1.2 mmol), PbO_2 (576 mg, 2.4 mmol) in a mixture of toluene (6 mL) and MeCN (1.5 mL) was stirred overnight at rt. Additional amounts of PbO_2 (288 mg, 1.72 mmol) were added and stirring was continued for the next 24 h. The dark green reaction mixture was passed through a silica gel plug (CH_2Cl_2), and the crude product was purified on a silica gel column (hexane / CH_2Cl_2 , 8:1) to give verdazyl **1b[n]** as a dark red waxy solid in yields ~80%. The solid was recrystallized several times from AcOEt or AcOEt with a few drops of MeCN.

Method B. A mixture of partially purified tetrazane **6b[n]** (0.5 mmol), $\text{K}_3\text{Fe}(\text{CN})_6$ (3 mmol), 0.5 M Na_2CO_3 (10 mL), $[\text{Bu}_4\text{N}]^+\text{Br}^-$ (cat) in CH_2Cl_2 (10 mL) was stirred overnight at rt. Next portion of $\text{K}_3\text{Fe}(\text{CN})_6$ (3 mmol) was added and stirring was continued until tetrazane **6b[n]** is no longer detectable on TLC. The black-green CH_2Cl_2 layer was separated, dried (Na_2SO_4), solvent was evaporated and the crude product was purified as described in Method A.

1,3,5-tri-(3',4',5'-Trioctyloxyphenyl)-6-oxoverdazyl (1b[8]). Method A. UV (hexane) λ_{max} (log ϵ) 209 (4.96), 274 (4.35), 3.44 (4.04), 486 (3.24), 614 (3.52) nm. Anal. Calcd for $\text{C}_{92}\text{H}_{159}\text{N}_4\text{O}_{10}$: C, 74.60; H, 10.82; N, 3.78. Found: C, 74.83; H, 10.91; N, 3.79.

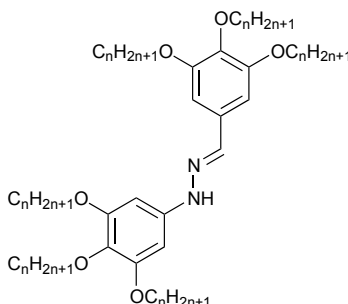
1,3,5-tri-(3,4,5-Tridecyloxyphenyl)-6-oxoverdazyl (1b[10]). Method B. Anal. Calcd for $\text{C}_{110}\text{H}_{195}\text{N}_4\text{O}_{10}$: C, 76.20; H, 11.34; N, 3.23. Found: C, 76.35; H, 11.28; N, 3.19.



Aldehydes 3b[n]. Aldehydes were obtained by alkylation of 3,4,5-trihydroxybenzaldehyde with appropriate alkyl bromide as described in literature^{7,8} in yields about 70%. Alternatively, 3,4,5-trioctyloxybenzaldehyde (**3b[8]**) was obtained in 70% yield from 1,2,3-trioctyloxy-4-bromobenzene⁹ by lithiation with *n*-BuLi and subsequent treatment with DMF according to a general procedure for preparation of aldehydes **3a[n]**.¹⁰

3,4,5-Trioctyloxybenzaldehyde (3b[8]).^{7,8} ¹H NMR (400 MHz, CDCl₃) δ 0.88 (t, *J*= 6.2 Hz, 9H), 1.23-1.40 (m, 24H), 1.44-1.52 (m, 6H), 1.75 (quint, *J*= 7.2 Hz, 2H), 1.83 (quint, *J*= 7.0 Hz, 4H), 4.03 (t, *J*= 6.5 Hz, 4H), 4.05 (t, *J*= 6.6 Hz, 2H), 7.08 (s, 2H), 9.83 (s, 1H).

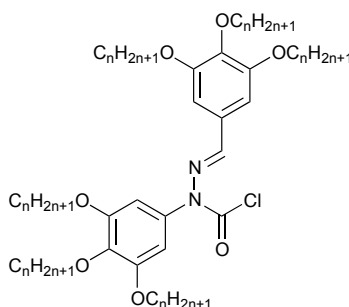
3,4,5-Tridecyloxybenzaldehyde (3b[10]).^{8,11} ¹H NMR (500 MHz, CDCl₃) δ 0.82 (t, *J*= 6.9 Hz, 9H), 1.23-1.40 (m, 36H), 1.44-1.52 (m, 6H), 1.75 (quint, *J*= 7.3 Hz, 2H), 1.83 (quint, *J*= 7.1 Hz, 4H), 4.03 (t, *J*= 6.4 Hz, 4H), 4.06 (t, *J*= 6.1 Hz, 2H), 7.08 (s, 2H), 9.83 (s, 1H).



Hydrazones 4b[n]. General Procedure. To a solution of crude 3,4,5-trialkyloxyphenylhydrazine¹² (**2b[n]**, 1.3 mmol) and 3,4,5-trialkyloxybenzaldehyde (**3b[n]**, 1.0 mmol) in THF (4 mL) 1 drop of AcOH was added. The mixture was refluxed for 1.5 h under Ar, cooled to rt, solvent was evaporated, and traces of AcOH removed on vacuum to give ~80% yield of crude hydrazone **4b[n]** (~90% pure), which was used for the next step without additional purification.

3,4,5-Trioctyloxybenzaldehyde 3,4,5-trioctyloxyphenylhydrazone (4b[8]). ^1H NMR (400 MHz, CDCl_3) δ (major signals) 0.88 (t, $J = 6.7$ Hz, 18H), 1.23-1.40 (m, 48H), 1.42-1.58 (m, 12H), 1.67-1.88 (m, 12H), 3.88 (t, $J = 6.6$ Hz, 2H), 3.98 (t, $J = 6.1$ Hz, 6H), 4.02 (t, $J = 6.4$ Hz, 4H), 6.32 (s, 2H), 6.84 (s, 2H), 7.40 (s, 1H), 7.55 (s, 1H).

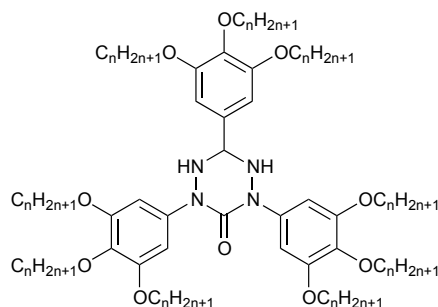
3,4,5-Tridecyloxybenzaldehyde 3,4,5-tridecyloxyphenylhydrazone (4b[10]). ^1H NMR (400 MHz, CDCl_3) (characteristic signals) δ 3.89 (t, 2H), 6.33 (s, 2H), 6.84 (s, 2H), 7.41 (s, 1H), 7.56 (s, 1H).



Carbamoyl chlorides 5b[n]. General Procedure. To a solution of hydrazone **4b[n]** (1.0 mmol) in dry CH_2Cl_2 (10 mL) pyridine (1.2 mmol) followed by triphosgene (297 mg, 1.0 mmol) were added under Ar. The mixture was stirred at ambient temperature for 4 hrs, 2% HCl was added, organic products were extracted (CH_2Cl_2), extracts dried (Na_2SO_4), and solvent evaporated. The crude product was purified on a short silica gel column (hexane / CH_2Cl_2 , 2:1) to give chlorides **5b[n]** as yellowish viscous oils in yields ~65%.

3,4,5-Trioctyloxybenzaldehyde α -chloroformyl-3',4',5'-trioctyloxyphenylhydrazone (5b[8]). ^1H NMR (400 MHz, CDCl_3) δ 0.84-0.92 (m, 18H), 1.19-1.35 (m, 48H), 1.40-1.53 (m, 12H), 1.68-1.76 (m, 4H), 1.80 (quint, $J = 6.5$ Hz, 8H), 3.93 (t, $J = 6.5$ Hz, 4H), 3.97 (t, $J = 6.6$ Hz, 2H), 3.98 (t, $J = 6.5$ Hz, 4H), 4.03 (t, $J = 6.4$ Hz, 2H), 6.39 (s, 2H), 6.84 (s, 2H), 7.22 (s, 1H); HRMS, calcd for $\text{C}_{62}\text{H}_{108}\text{ClN}_2\text{O}_7$ (M+1): m/z 1027.7840; found m/z 1027.7828.

3,4,5-Tridecyloxybenzaldehyde α -chloroformyl-3',4',5'-tridecyloxyphenylhydrazone (5b[10]). ^1H NMR (400 MHz, CDCl_3) (characteristic signals) δ 6.39 (s, 2H), 6.84 (s, 2H), 7.22 (s, 1H). Molecular ion was not observed.



Tetrazanes 6b[n]. General Procedure. To a solution of carbamoyl chloride **5b[n]** (1.0 mmol) in dry benzene (30 mL) a solution of freshly prepared 3,4,5-trialkyloxyphenylhydrazine¹² (**2b[n]**, 1.2 mmol) and Et_3N (1.3 mmol) in dry benzene (10 mL) was added. The mixture was stirred for 2 h at 50 °C. A 2% solution of HCl was added, organic products were extracted (CH_2Cl_2), extracts dried (Na_2SO_4), and solvents evaporated. The crude product was purified on a short silica gel column (hexane / CH_2Cl_2 , 2:1) to give partially purified tetrazane **6b[n]** as a tan viscous oil or soft solid in yields ~45%. Molecular ions in MS were not observed.

2,4,6-Tri(3,4,5-trioctyloxyphenyl)-1,2,4,5-tetrazane-3-one 6b[8]. Yellow-brownish viscous oil (~60% of yield based on mass and NMR): ^1H NMR (400 MHz, CDCl_3) δ 0.84-0.94 (m, 27H), 1.22-1.37 (m, 72H), 1.38-1.52 (m, 18H), 1.66-1.83 (m, 18H), 3.78 (t, $J = 6.4$ Hz, 4H), 3.90 (t, $J = 6.7$ Hz, 6H), 3.94 (t, $J = 6.6$ Hz, 8H), 4.67 (d, $J = 9.1$ Hz, 2H), 5.42 (t, $J = 8.7$ Hz, 1H), 6.69 (s, 2H), 6.84 (s, 4H).

2,4,6-Tri(3,4,5-tridecyloxyphenyl)-1,2,4,5-tetrazane-3-one 6b[10]. ^1H NMR (400 MHz, CDCl_3) δ 0.89 (t, $J = 6.6$ Hz, 27H), 1.22-1.38 (m, 108H), 1.39-1.51 (m, 18H), 1.66-1.85 (m, 18H), 3.78 (t, $J = 6.3$ Hz, 4H), 3.91 (t, $J = 6.7$ Hz, 6H), 3.94 (t, $J = 6.5$ Hz, 8H), 4.70 (brs, 2H), 5.42 (brs, 1H), 6.70 (s, 2H), 6.85 (s, 4H).

2. Thermal analysis

Thermal analysis was performed on a TA 2920 DSC. In a typical experiment, both compounds were analyzed in multiple heating/cooling cycles with heating/cooling rates of 5 K min⁻¹. The isotropic-columnar transition for **1b[10]** was analyzed using variable cooling rates (Fig. S1).

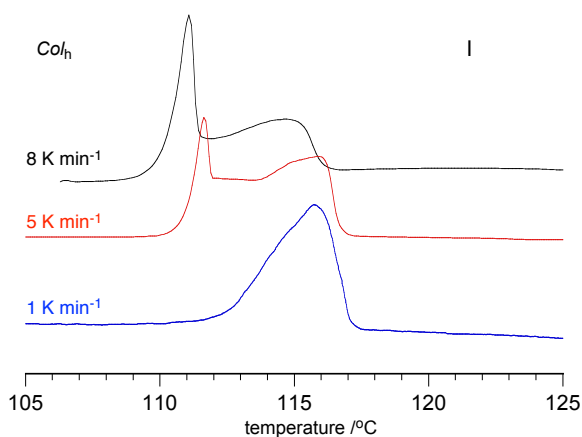


Figure S1. Isotropic–columnar phase transition recorded on cooling for **1b[10]** at various cooling rates.

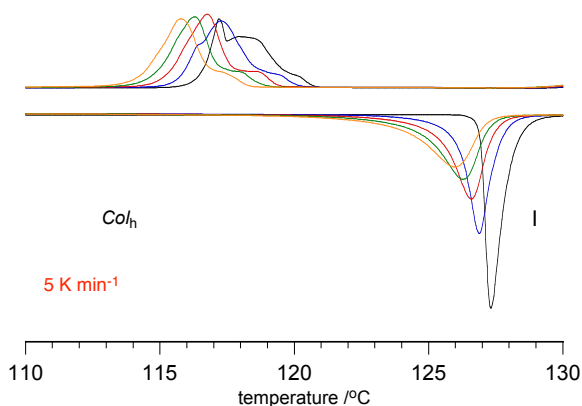


Figure S2. Isotropic–columnar phase transition recorded for **1b[8]** during 5 cycles of heating and cooling in a range of 100–135 °C at 5 K min⁻¹.

3. Optical textures

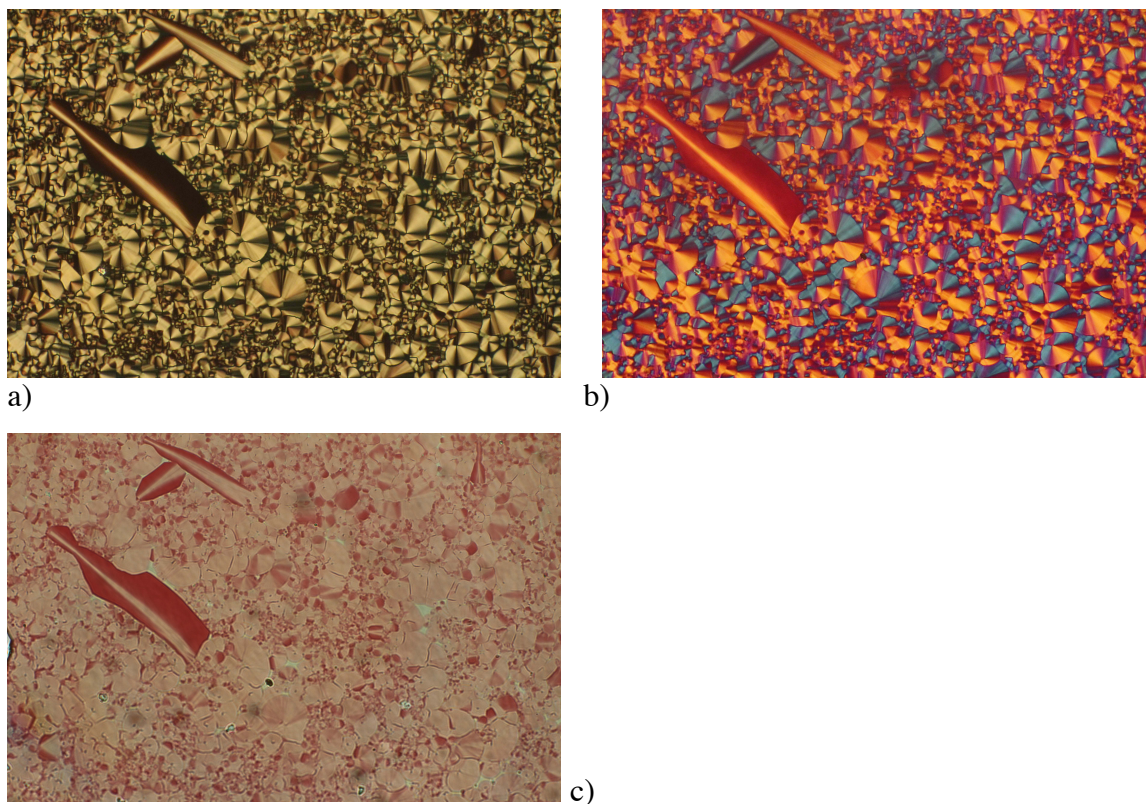


Figure S3. Photomicrograph of **1b[10]** with crossed polarizers (a), crossed polarizers and lambda plate inserted at 45 deg to the polarizer direction (b), and no polarizers.

4. Electronic absorption spectra

UV-vis spectra for **1b[8]** were recorded in spectroscopic grade hexane at concentration of $1-10 \times 10^{-6}$ M. Extinction coefficients were obtained by fitting the maximum absorbance at 260 nm against concentration in agreement with Beer's law.

The temperature-dependent visible spectra for **1b[10]** were obtained every 1 or 2 K on heating and cooling using a hot-stage mounted in a UV spectrometer. The sample was allowed to equilibrate for 3 min after each change of temperature. A plot for **1b[10]** is shown in Figure S4.

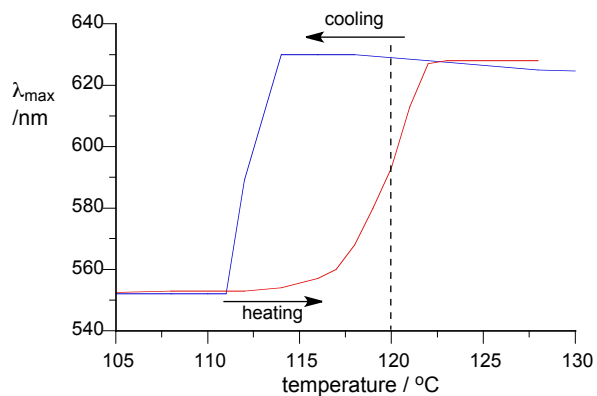


Figure S4. Temperature dependent lowest energy absorption maximum of **1b[10]**.

5. Powder XRD measurements

X-ray diffraction experiments were performed with Bruker D8 GADDS (Cu $K\alpha$ radiation, Göbel mirror, point collimator, Vantec 2000 area detector) equipped with a modified Linkam heating stage. Samples were prepared in a form of a thin film or a droplet on heated surface. The X-ray beam was incident nearly parallel to sample surface, and resulting XRD patterns were recorded as a function of temperature.

Results are shown in Figures S5–S8 and Tables S1 and S2.

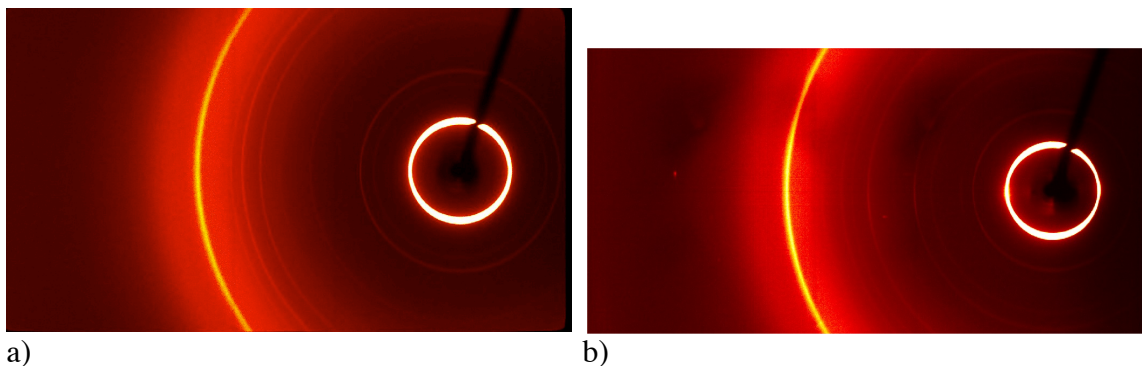


Figure S5. Wide angle X-ray diffraction pattern for **1b[8]** at 115 °C (a) and for **1b[10]** obtained at 30 °C (b).

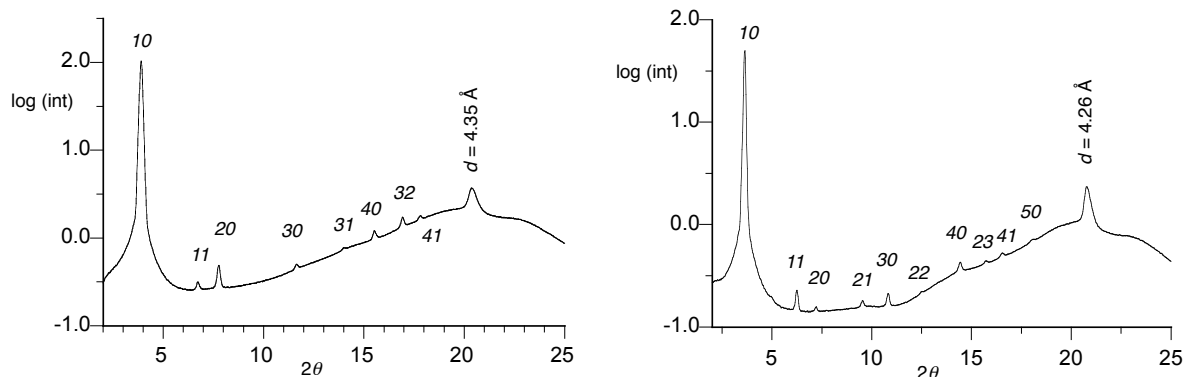


Figure S6. 2D pattern for **1b[8]** at 115 °C (left) and for **1b[10]** at 30 °C (right). Signals are indexed assuming 2D hexagonal lattice.

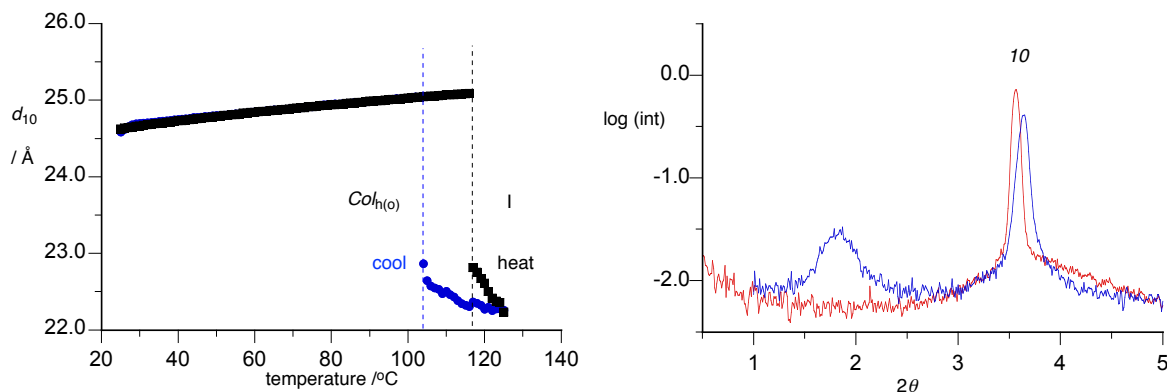


Figure S7. Temperature dependence of the position of d_{10} reflection in the Col_h phase and diffused signal in the Iso phase for **1b[10]** recorded on heating (black) and cooling (blue).

Figure S8. Small angle XRD pattern for **1b[10]** recorded at 50 °C (red) and at 5 °C (blue). In low temperature additional broad signal appears reflecting short-range density modulations with the periodicity twice the periodicity of (10)

Table S1. X-ray diffraction data for **1b[8]**.

Sample	Temp /°C	Phase	Miller indices <i>hk</i>	d_{meas} /Å obs	d_{calcd} /Å calcd	Cell parameter /Å
1b[8]	115	<i>Col_{h(o)}</i>	10	22.81	22.81	<i>a</i> = 26.35
			11	13.18	13.17	
			20	11.42	11.41	
			30	7.61	7.60	
			31	6.34	6.33	
			40	5.71	5.70	
			32	5.24	5.23	
			41	4.98	4.98	
			diff	4.6		
			sharp	4.35		
diff	4.0					

Table S2. X-ray diffraction data for **1b[10]**.

Sample	Temp /°C	Phase	Miller indices <i>Hk</i>	d_{meas} /Å obs	d_{calcd} /Å calcd	Cell parameter /Å
1b[10]	30	<i>Col_h</i>	10	24.56	24.56	<i>a</i> = 28.35
			11	14.22	14.18	
			20	12.31	12.28	
			21	9.30	9.28	
			30	8.20	8.18	
			22	7.11	7.09	
			40	6.15	6.14	
			23	5.65	5.63	
			41	5.37	5.36	
			50	4.93	4.91	
			diff	4.47		
			sharp	4.26		
			diff	3.87		

6. Photoconductivity measurements and data

The charge carrier mobility was measured for **1b[8]** by the TOF (time-of-flight) method using a nitrogen gas laser (Nippon Laser, 800 ps pulse at $\lambda = 337$ nm) and a polarizing microscope with a hot stage. The cell was mounted on a handmade hot stage, and electric bias was applied by battery cells. Depending on the polarity of the applied

field (40 kV or 50 kV), positive or negative charge carriers were moving through the sample, causing displacement photocurrent, which is detected on a digital oscilloscope with a commercially available current amplifier (DHPCA-100, FEMTO). A schematic diagram of the experimental setup is shown in Figures S9 and S10 and the data in Table S3. Figure S11 shows a typical texture of a sample **1b[8]** that was used for the measurements.

Thickness of the cells used for TOF measurements was 2.3, 5.2, and 18.6 μm and the electrodes in the thickest cell were covered with a 300 nm-thick layer of SiO_2 . The cells were filled with isotropic material by capillary forces. The material was rapidly cooled to a columnar phase. Polarized optical microscopy showed a highly birefringent texture practically with no homeotropic domains. Slow cooling in magnetic field did not result in sample alignment. Optical density of the 2.3 μm sample at 337 nm was 0.72.

- Dark current measurements in a range of 25–90 $^{\circ}\text{C}$ gave the value of 10^{-14} – 10^{-12} S cm^{-1} with an activation energy of about 0.9 eV.
- Photoconductivity of **1b[8]** in a 5.2 μm thick cell (area of the electrode: 0.16 cm^2): 3.6×10^{-15} S cm^{-1} at 25 $^{\circ}\text{C}$ and 6.0×10^{-13} S cm^{-1} at 90 $^{\circ}\text{C}$.

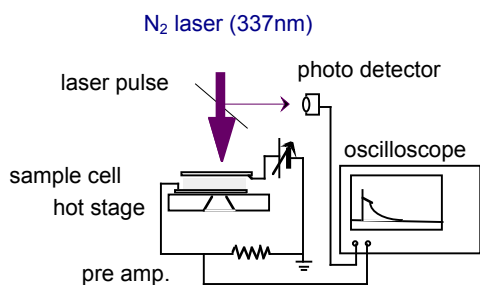


Figure S9. Schematic diagram of the experimental apparatus (TOF method).

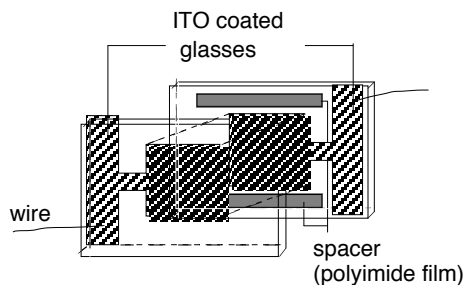


Figure S10. Sandwich-type cell for photoconductivity measurements.

Table S3. Positive (μ_h) charge mobilities in **1b[8]** at 40 kV measured on cooling

Temperature / °C	Mobility $\times 10^{-3}$ /cm ² V ⁻¹ s ⁻¹
120	3.44
110	3.02
100	3.37
90	3.38
80	2.87
70	2.87
60	3.34
50	3.23
40	3.14

The estimated uncertainty of charge mobility values is about 20%, which was based on the assumed 10% of uncertainty of the cell thickness and the depth of light penetration of the sample.



Figure S11. Texture of a typical sample of **1b[8]** used for photocurrent generation studies.

7. Magnetization measurements

Experiments were conducted using SQUID magnetometer (Quantum Design MPMS-XL-7T).

A small fresh sample of **1b[8]** ($m = 4.73$ mg, 3.19×10^{-6} mol), prepared with PbO₂, was placed in a polycarbonate capsule fitted in a plastic straw. The sample was subjected to heating and cooling experiments at 0.05 T in a range of temperatures of between 2 K and 400 K at a rate of 1 K min⁻¹.

The signal at high temperature was relatively weak and was measured once at

each temperature in the sweep mode without averaging. In the range of 40–100 K the SQUID signal changes from negative to positive (goes through 0) and magnetization M could not be derived.

The diamagnetic correction was established by fitting the magnetization data to a χ_{mol} *vs* $1/T$ plot (Curie plot), which for an ideal paramagnet is required to go through 0. After diamagnetic correction, the Curie constant was found to be $C = \chi_{\text{m}}T$ equal $0.317(1) \text{ cm}^3 \text{ K mol}^{-1}$ at a temperature range 200–360 K (Figure S11). Below 200 K the plot shows increasing AF interactions (Figure S12). The established diamagnetic correction also contains correction for magnetic field strength uncertainty, which might be up to 5% at 500 Oe.

The molar susceptibility χ_{m} was converted to dimensionless μ_{eff} according to the equation $\mu_{\text{eff}} = 2.828 \cdot (\chi_{\text{m}}T)^{1/2}$ (Hoppeè, J. I. *J. Chem. Ed.* **1972**, *49*, 505) and a plot *vs* T is shown in Figure S14.

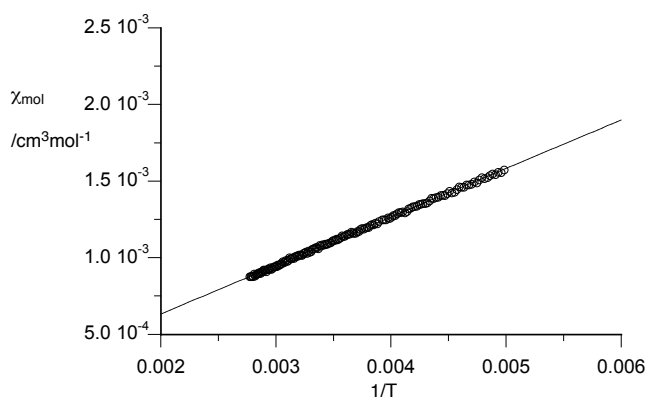


Figure S12. Paramagnetic molar susceptibility χ_{m} *vs* $1/T$ plot after diamagnetic correction. $C = 0.317(1) \text{ cm}^3 \text{ K mol}^{-1}$. $H = 500 \text{ Oe}$

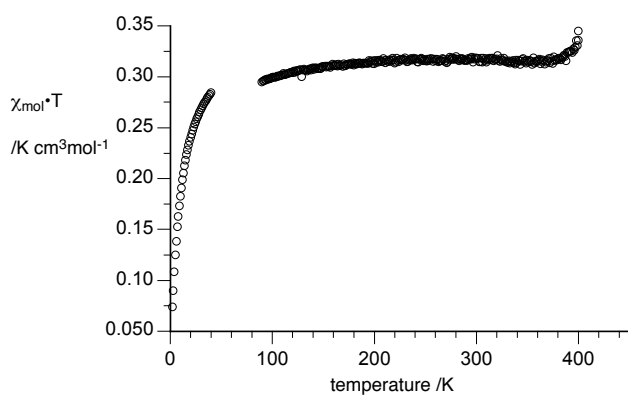


Figure S13. $\chi_{\text{m}} \cdot T$ *vs* T plot. $H = 500 \text{ Oe}$.

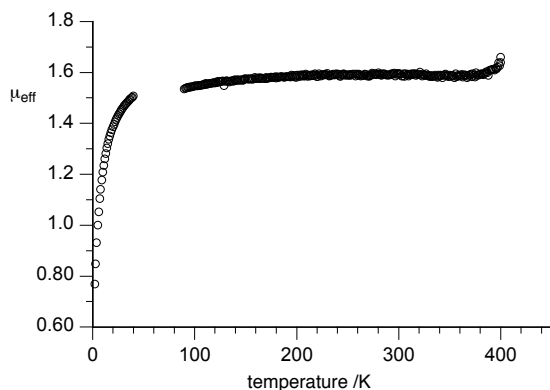


Figure S14. μ_{eff} *vs* T plot. H = 500 Oe.

8. Electrochemistry

Electrochemical analysis of **1b[8]** was conducted under argon in dry CH_2Cl_2 containing freshly dried $[\text{Bu}_4\text{N}]^+[\text{PF}_6]^-$ (50 °C, P_2O_5 , vacuum, overnight) as the supporting electrolyte (0.1 M) and a glassy carbon working electrode with Ag/AgCl pseudo electrode as reference. The scanning rate was 0.1 V/s. Peak potentials were referenced to the Fc/Fc⁺ couple by adding small amounts of ferrocene to the solution, which was assumed to be +0.475 V versus SCE (CH_2Cl_2 , 0.1 M $[\text{Bu}_4\text{N}]^+[\text{ClO}_4]^-$).¹ A typical voltammogram for **1b[8]** is shown in Figure S15 and compared to that of its sulfur analog **1a[8]** recorded under identical conditions.

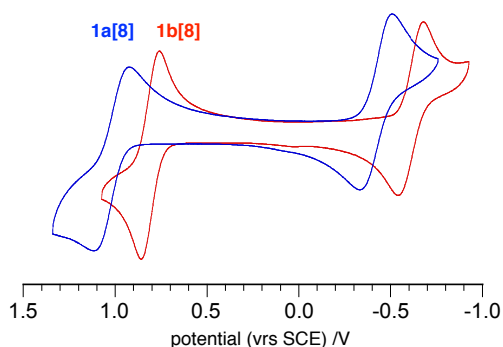


Figure S15. The cyclic voltammograms of **1a[8]** (blue) and **1b[8]** (red): 1 mM, $[\text{Bu}_4\text{N}]^+[\text{PF}_6]^-$, 0.1 M, 100 mV/s.

9. Molecular modeling and computational details

Geometry optimizations were carried out using Universal Force Field algorithm supplied with Cerius2 suite of programs. The structure of **1b[8]** was set in the most

extended conformation as the initial guess, optimized and perturbed a number of times until a minimum energy was obtained. The result is shown in Figure S16.

Quantum-mechanical calculations were carried out at the UB3LYP/6-31G(d,p) level of theory using Gaussian 09 suite of programs.² Geometry optimizations were undertaken using default convergence limits and without symmetry constraints. Vibrational frequencies were used to characterize the nature of the stationary points. Zero-point energy (ZPE) corrections were scaled by 0.9806.³

Following general recommendations,⁴ energy for ion formation was derived as the difference of SCF energies of individual species computed using the 6-31+G(d,p) basis set at the geometries obtained with the 6-31G(d,p) basis set (single point calculations). Thermodynamic corrections were obtained using the 6-31G(d,p) basis set.

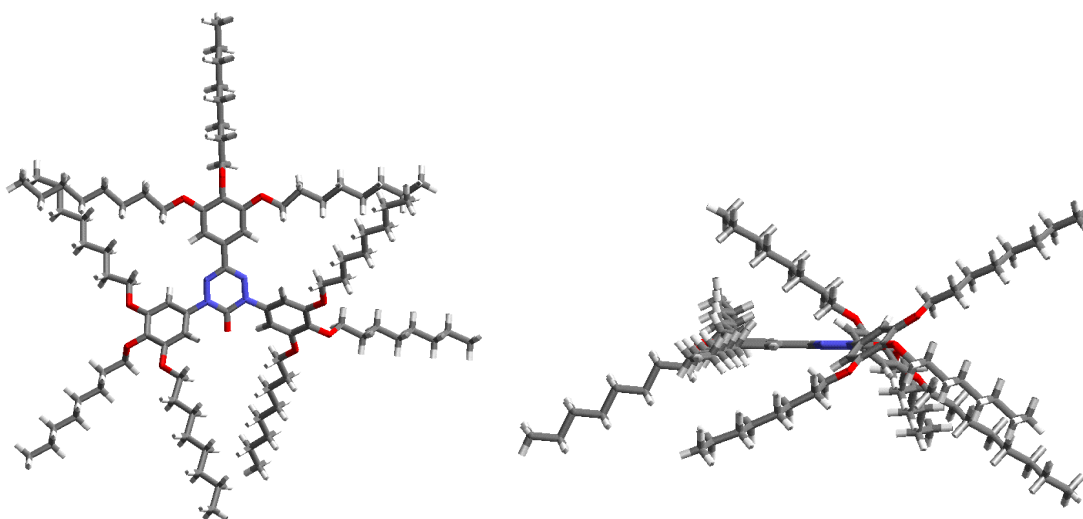


Figure S16. Two views of a molecule of **1b[8]** optimized with UFF algorithm. All alkyl chains are in the *trans* conformation.

Electronic excitation energies for **1b[1]** in vacuum were obtained at the UB3LYP/6-31G(d,p) level using the time-dependent DFT method⁵ supplied in the Gaussian package.

10. Disproportionation energy

Ionization potentials I_p and electron affinities E_a for **1a[1]**, **1b[1]** and phenalenyl were calculated according to Scheme S1 and results are shown in Table S4.

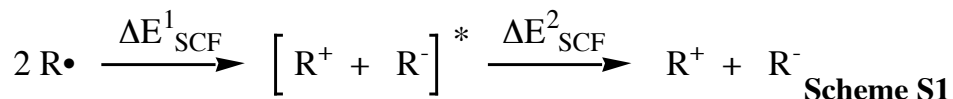


Table S4. Calculated (B3LYP/6-31+G(d,p)//B3LYP/6-31G(d,p)) parameters for selected radicals in vacuum.

	$I_p(\text{vert})$ [eV] ^a	E_a [eV]	ΔE^1_{SCF} ^b [kcal/mol]	ΔE^2_{SCF} ^b [kcal/mol]	$\Sigma \Delta E_{SCF}$ ^b [kcal/mol]
1a[1]	6.65	2.30	102.9	-8.8	94.1
1b[1]	6.50	1.84	107.5	-15.2	92.3
 PHEN	6.07	1.24	116.1	-0.7	115.4

^a Calculated value scaled by 0.984 (see ref⁶). ^b ΔE^1_{SCF} is the electron transfer energy and ΔE^2_{SCF} is the relaxation energy. $\Sigma \Delta E_{SCF}$ represents the energy of the overall disproportionation process (Scheme S1).

11. Partial data for TD-DFT calculation (B3LYP/6-31G(d,p)) for 1b[1]

Excitation energies and oscillator strengths:

```
Excited State 1: 2.028-A      2.0192 eV  614.01 nm  f=0.0731
<S**2>=0.778
 158A ->159A      -0.12199
 158A ->160A      -0.10337
 150B ->158B       0.11329
 157B ->158B      0.96577
```

This state for optimization and/or second-order correction.

Total Energy, E(TD-HF/TD-KS) = -2095.97900447

Copying the excited state density for this state as the 1-particle RhoCI density.

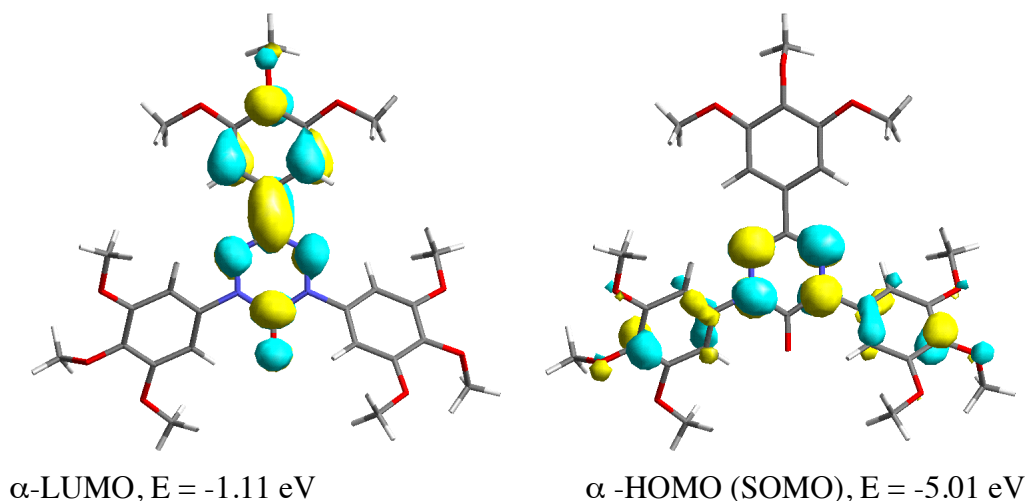
```
Excited State 2: 2.075-A      2.4130 eV  513.82 nm  f=0.0480
<S**2>=0.827
 158A ->159A      -0.21386
 151B ->158B      -0.15964
 154B ->158B      -0.10715
 155B ->158B       0.11502
 156B ->158B      0.92556
```

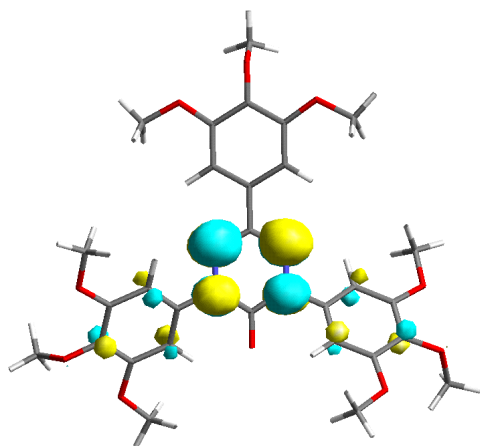
```
Excited State 3: 2.121-A      2.4543 eV  505.17 nm  f=0.0432
<S**2>=0.874
 158A ->161A      -0.10493
 152B ->158B       0.14003
 155B ->158B      0.95141
 156B ->158B      -0.12615
```

```
Excited State 4: 2.061-A      2.4845 eV  499.03 nm  f=0.0016
<S**2>=0.812
 154B ->158B      0.98271
 156B ->158B       0.11600
```

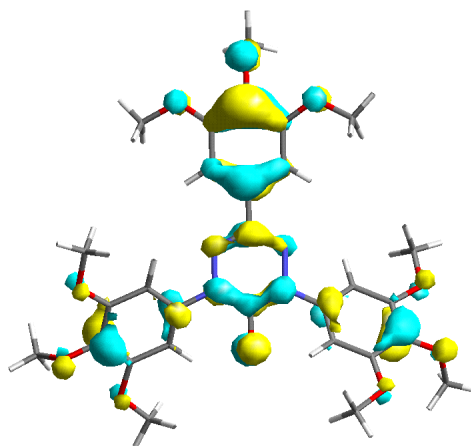
Excited State	5:	2.063-A	2.5311 eV	489.84 nm	f=0.0076
<S**2>=0.814					
152B ->158B		0.83172			
153B ->158B		0.51881			
155B ->158B		-0.15783			
Excited State	6:	2.048-A	2.5765 eV	481.21 nm	f=0.0001
<S**2>=0.799					
152B ->158B		-0.52395			
153B ->158B		0.84328			
Excited State	7:	2.049-A	2.7375 eV	452.91 nm	f=0.0069
<S**2>=0.800					
144B ->158B		-0.13496			
147B ->158B		-0.31954			
149B ->158B		0.12092			
150B ->158B		-0.23389			
151B ->158B		0.85417			
154B ->158B		-0.10152			
156B ->158B		0.15774			
Excited State	8:	2.041-A	2.8985 eV	427.75 nm	f=0.0041
<S**2>=0.792					
152A ->159A		0.16440			
158A ->159A		0.91472			
158A ->165A		0.10286			
150B ->158B		-0.11482			
156B ->158B		0.25462			
157B ->158B		0.12678			

Selected molecular orbitals involved in these transitions are shown in Figure S17.

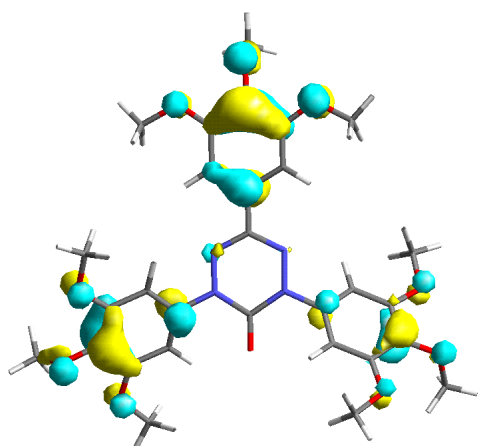




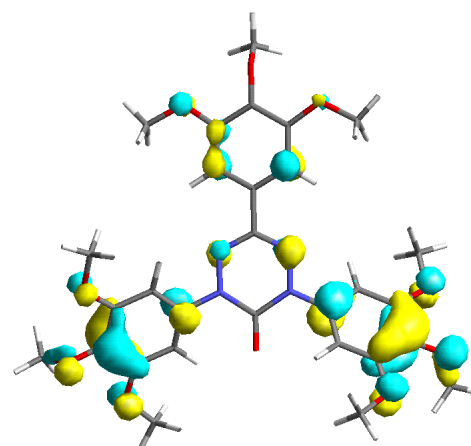
β -LUMO, $E = -2.76$ eV



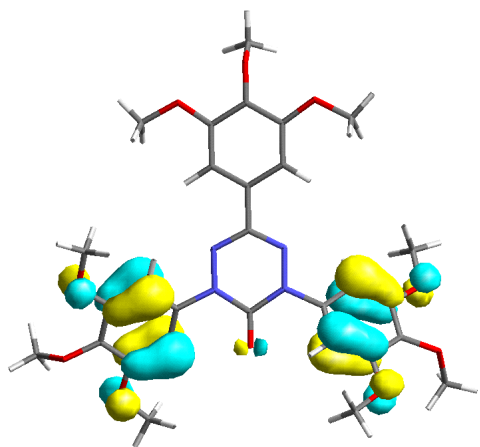
β -HOMO, $E = -5.52$ eV



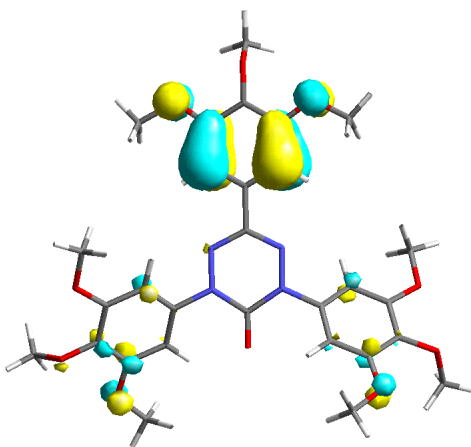
β -HOMO-1, $E = -5.84$ eV



β -HOMO-2, $E = -5.86$ eV



β -HOMO-3, $E = -5.94$ eV



β -HOMO-4, $E = -5.97$ eV

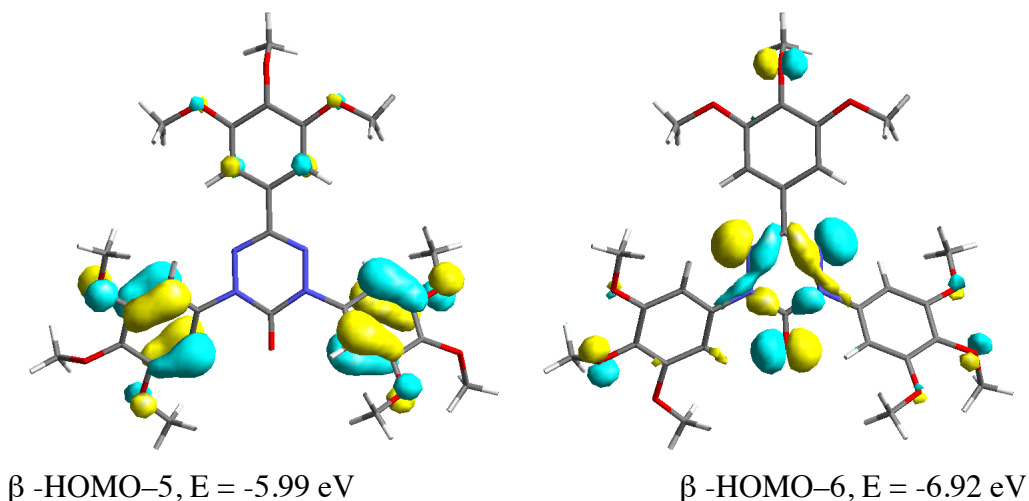


Figure S17. Contours and energies of selected orbitals involved in low energy excitations in **1b[1]**.

12. Archive data for B3LYP/6-31G(d,p) optimizations of **1b[1]**

```
1\1\GINC-OCTOPUS\FOpt\UB3LYP\6-31G(d,p)\C29H33N4O10(2)\PIOTR\16-Nov-20
11\0\#\#P B3LYP/6-31G(d,p) FOpt Geom(NoAngle, noDistance) fcheck freq=n
oraman\1,3,5-(3,4,5-MeOphenyl)-6-oxoverdazyl, C1\0,2\O,-0.0621290594
,-0.5197023953,0.0730087124\C,-0.024801063,-0.2280759499,1.2564537525\
N,1.1666267504,-0.1400466245,1.9913766149\N,1.2256409684,0.2086402802,
3.3129166548\C,0.0568983977,0.4234807479,3.9155208874\N,-1.1480708619,
0.3515544799,3.3509420331\N,-1.1699541074,0.0515776475,2.016747988\C,-
2.4874435072,-0.0712729003,1.4543303311\C,-2.7474635592,0.3202968131,0
.1388263337\C,-4.0529924142,0.2125388405,-0.3508282226\C,-5.0927302628
,-0.2635614568,0.4669578281\C,-4.8034803184,-0.6544762729,1.7863624197
\C,-3.5021076976,-0.55328083,2.2861700673\C,0.1012886246,0.7796759617,
5.357363623\C,-1.0468675288,1.2791738755,5.9835667064\C,-1.0038580246,
1.6180853306,7.33919354\C,0.1885866621,1.4692411052,8.0701739334\C,1.3
308737938,0.9532410126,7.4318067826\C,1.2909413161,0.6134512937,6.0770
108702\C,2.447951363,-0.3065343764,1.3604719719\C,3.5040245383,0.48220
01352,1.8260099935\C,4.7746348522,0.3210187438,1.2662880949\C,4.986448
412,-0.6110257577,0.2349136431\C,3.9096319767,-1.3980230882,-0.2092187
257\C,2.6370426581,-1.2558304547,0.3528503832\O,-6.384303573,-0.302071
2307,0.0134842806\O,6.2155742801,-0.6984720803,-0.3625153785\H,-3.2594
615007,-0.833193218,3.3003759832\O,-5.8628106999,-1.1275027158,2.50101
97412\C,-5.6395421623,-1.516552129,3.8467072505\H,-6.6078784584,-1.844
5231107,4.2271903197\H,-4.9237144585,-2.3456033809,3.9180058309\H,-5.2
768127177,-0.6787718051,4.4557839884\C,-6.7019301346,-1.4362707585,-0.
7964157809\H,-6.5635863573,-2.3701473221,-0.2379779904\H,-7.754333513,
-1.3326383048,-1.0685300009\H,-6.0920370419,-1.4566537354,-1.706182194
1\O,-4.4205053524,0.5536451934,-1.6187002579\H,-1.9463442974,0.6799289
666,-0.4853841489\H,2.1587815696,0.2177042726,5.5686411309\C,-3.419650
5359,1.0506145504,-2.4961871604\H,-2.983405881,1.9851072408,-2.1221753
282\H,-2.6181848301,0.3184399905,-2.65378394\H,-3.9246051254,1.2448131
679,-3.4433461442\O,2.4302930289,0.8205012331,8.2293951419\C,3.6245649
091,0.3288502347,7.6418910241\H,4.3680223183,0.3180423512,8.4401982064
\H,3.4978115749,-0.6888772737,7.251331358\H,3.9743866358,0.9805977135,
6.8312920734\O,0.2448324496,1.8756265623,9.3770080513\C,0.0432855999,0
```

.8351866586,10.3352888694\H,0.1126515567,1.3058815742,11.3181707676\H,
-0.9486012697,0.3810982556,10.2216851848\H,0.8153387963,0.0621267764,1
0.2487663736\O,-2.0626219445,2.1059506786,8.046029704\H,-1.9502232068,
1.3961308255,5.4016717511\H,1.8063767809,-1.8483451309,0.0071154729\C,
-3.278778749,2.3326533031,7.3511328552\H,-3.1502902192,3.0548061607,6.
535385953\H,-3.6933307207,1.402411379,6.9413708113\H,-3.9721607834,2.7
407909544,8.0878224526\O,4.2085312688,-2.2866131383,-1.1993899532\C,3.
1514755489,-3.0663240869,-1.7409975456\H,2.7164054755,-3.7376666895,-0
.9897309058\H,2.3584512048,-2.4348712146,-2.1590511675\H,3.5990716253,
-3.6616294075,-2.5379586516\C,7.0270886939,-1.7840536956,0.090877702\H
,6.5505615925,-2.7487091902,-0.1156653992\H,7.9648933466,-1.7176513659
, -0.4645100841\H,7.2364758588,-1.6980937703,1.1642033257\O,5.874223005
,1.0284194143,1.6493332333\H,3.320145299,1.1883349643,2.6216216972\C,5
.7137808375,2.0236798417,2.6477541952\H,6.6993194643,2.4709148746,2.78
43068562\H,5.0045397469,2.8003398688,2.3354792518\H,5.376683156,1.5944
685872,3.6002269771\Version=EM64L-G09RevA.02\State=2-A\HF=-2096.05321
03\S2=0.772626\S2-1=0.\S2A=0.750245\RMSD=3.626e-09\RMSF=1.600e-06\Dipo
le=0.1055986,-1.1993507,0.2654743\Quadrupole=-2.3578312,2.2960605,0.06
17708,1.4339123,3.98176,-2.9366495\PG=C01 [X(C29H33N4O10)]\@

12. References

- (1) Noviadri, I.; Brown, K. N.; Fleming, D. S.; Gulyas, P. T.; Lay, P. A.; Masters, A. F.; Phillips, L. *J. Phys. Chem. B* **1999**, *103*, 6713.
- (2) Gaussian 09, Revision A.02, M. J. Frisch, G. W. Trucks, H. B. Schlegel, G. E. Scuseria, M. A. Robb, J. R. Cheeseman, G. Scalmani, V. Barone, B. Mennucci, G. A. Petersson, H. Nakatsuji, M. Caricato, X. Li, H. P. Hratchian, A. F. Izmaylov, J. Bloino, G. Zheng, J. L. Sonnenberg, M. Hada, M. Ehara, K. Toyota, R. Fukuda, J. Hasegawa, M. Ishida, T. Nakajima, Y. Honda, O. Kitao, H. Nakai, T. Vreven, J. A. Montgomery, Jr., J. E. Peralta, F. Ogliaro, M. Bearpark, J. J. Heyd, E. Brothers, K. N. Kudin, V. N. Staroverov, R. Kobayashi, J. Normand, K. Raghavachari, A. Rendell, J. C. Burant, S. S. Iyengar, J. Tomasi, M. Cossi, N. Rega, J. M. Millam, M. Klene, J. E. Knox, J. B. Cross, V. Bakken, C. Adamo, J. Jaramillo, R. Gomperts, R. E. Stratmann, O. Yazyev, A. J. Austin, R. Cammi, C. Pomelli, J. W. Ochterski, R. L. Martin, K. Morokuma, V. G. Zakrzewski, G. A. Voth, P. Salvador, J. J. Dannenberg, S. Dapprich, A. D. Daniels, O. Farkas, J. B. Foresman, J. V. Ortiz, J. Cioslowski, and D. J. Fox, Gaussian, Inc., Wallingford CT, 2009.
- (3) Scott, A. P.; Radom, L. *J. Phys. Chem.* **1996**, *100*, 16502.
- (4) Clark, T.; Chandrasekhar, J.; Spitznagel, G. W.; Schleyer, P. v. R. *J. Comput. Chem.* **1983**, *4*, 294.
- (5) Stratmann, R. E.; Scuseria, G. E.; Frisch, M. J. *J. Chem. Phys.* **1998**, *109*, 8218.
- (6) Kaszynski, P. *J. Phys. Chem. A*, **2001**, *105*, 7626.
- (7) Holst, H. C.; Pakula, T.; Meier, H. *Tetrahedron* **2004**, *60*, 6765.
- (8) Nowak-Król, A.; Gryko, D.; Gryko, D. T. *Chem. Asian J.* **2010**, *5*, 904.
- (9) Yasuda, T.; Shimizu, T.; Liu, F.; Ungar, G.; Kato, T. *J. Am. Chem. Soc.* **2011**, *133*, 13437.
- (10) Jankowiak, A.; Dębska, Z.; Kaszyński, P.; Romański, J. *J. Sulfur Chem.* **2012**, *33*, 1.

- (11) Kretschmann, H.; Müller, K.; Kolshorn, H.; Schollmeyer, D.; Meier, H. *Chem. Ber.* **1994**, *127*, 1735.
- (12) Jankowiak, A.; Kaszyński, P. *Beils. J. Org. Chem.* **2012**, *8*, 275.